nature structural & molecular biology

© 2005 Nature Publishing Group http://www.nature.com/nsmb

Hemifusion in SNARE-mediated membrane fusion

Yibin Xu[1,3], Fan Zhang[1,3], Zengliu Su[1], James A McNew[2] & Yeon-Kyun Shin[1]

SNAREs are essential for intracellular membrane fusion. Using EPR, we determined the structure of the transmembrane domain (TMD) of the vesicle (v)-SNARE Snc2p involved in trafficking in yeast. Structural features of the TMD were used to design a v-SNARE mutant in which about half of the TMD was deleted. Liposomes containing this mutant induced outer leaflet mixing but not inner leaflet mixing when incubated with liposomes containing target membrane (t)-SNAREs. Hemifusion was also detected with wild-type SNAREs when low protein concentrations were reconstituted. Thus, these results show that SNARE-mediated fusion can transit through a hemifusion intermediate.

A wide variety of important life processes, including viral entry, fertilization and intracellular transport, depend on membrane fusion mediated by specialized proteins[1]. Progress in determining three-dimensional structures of several such proteins improved the understanding of how the proteins might bring about the apposition of two membranes[2–4]. However, the specific transitions that lipids experience as two membranes become merged into a single bilayer is still unclear[5].

It is generally believed that viral-cell membrane fusion for class I viruses proceeds through an intermediate called hemifusion[6] before the formation of a fusion pore. During hemifusion, two membranes are merged at the level of the outer phospholipid monolayer, while the inner monolayers retain their original integrity. Hemifusion has been identified for membrane fusion induced by modified class I viral fusion proteins including mutant influenza hemagglutinin[7–9], and it has been directly observed with model membranes[10].

In eukaryotic cells, all membrane fusion in the secretory pathway is mediated by SNARE proteins[11,12], and the specific pairing of SNAREs between membranes is sufficient to drive membrane fusion in a minimal system[13,14]. Although class I viral fusion proteins and SNAREs share structural similarity[2], some have suggested that intracellular membrane fusion might work differently. One proposed alternative is that formation of SNARE complex connects two preformed, complementary proteinaceous pores. In one case, the pore is predicted to be made of the TMDs of individual SNAREs[15], contrary to earlier hypothetical models proposing a hemifusion-like intermediate[16,17], whereas other models invoke different pore-forming proteins[18]. The pore model predicts a protein-lined channel rather than lipidic intermediates[6] and therefore does not require hemifusion as a fusion intermediate because the pore is already established at the onset of membrane fusion. Contrary to this view, it has been shown that full fusion can still be achieved when the SNARE TMDs are replaced with a long lipid anchor[19].

Undoubtedly, TMDs of SNAREs are central components of the fusion machinery. To investigate the roles of SNARE TMDs in membrane fusion, we determined the structure of the TMD of the v-SNARE Snc2p involved in post-Golgi trafficking in yeast, using site-directed spin-labeling EPR[20]. The predicted structure was used to design a deletion mutant of Snc2p that arrests the fusion process at hemifusion. Furthermore, careful analysis of fusion driven by wild-type SNAREs revealed a hemifusion intermediate at dilute protein concentrations. These results are in apparent disagreement with the protein pore–based models[15,18], but are consistent with a hemifusion-based lipidic fusion pore model[5,6].

RESULTS

Site-directed spin-labeling EPR on v-SNARE Snc2p

To investigate the transmembrane structure of yeast v-SNARE Snc2p, native residues were replaced one by one with cysteines derivatized with methanethiosulfonate spin label (MTSSL). The spin-labeling efficiency was >80% for all the mutants. Each spin-labeled mutant was independently reconstituted into donor phospholipid vesicles containing 1-palmitoyl-2-dioleoyl-*sn*-glycero-3-phosphatidylcholine (POPC), 1,2-dioleoyl-*sn*-glycero-3-phosphatidylserine (DOPS), 1,2-dioleoyl-*sn*-glycero-3-phosphoethanolamine-N-(7-nitro-2-1,3-benzoxadiazol-4-yl) (NBD-PE) and 1,2-dioleoyl-*sn*-glycero-3-phosphoethanolamine-*N*-(lissamine rhodamine B sulfonyl) (rhodamine-PE) in the molar ratio of 72:25:1.5:1.5. The functionality of the spin-labeled Snc2p mutants was determined by *in vitro* fusion experiments with vesicles containing the t-SNARE complex Sso1pHT–Sec9c to monitor total lipid mixing[13,14]. All mutants showed at least 60% of the fusion activity of wild-type Snc2p (**Fig. 1a**).

Fourteen out of twenty mutants showed relatively narrow EPR spectra (**Fig. 1b**), typical of fully lipid-exposed nitroxides[21]. However, six mutants (V98C, I100C, L103C, I107C, P109C and V111C) exhibited noticeably broader spectral components (arrows in **Fig. 1b**), indicative of partial tertiary contacts[22], most likely with neighboring TMDs. The presence of two spectral components suggests that there is equilibrium between the monomer and the oligomers. In the helical wheel diagram (**Fig. 1c**), positions 100, 103, 107 and 111 are located on one side of the helix, suggesting that this may be an interacting face of the helix. We also

[1]Department of Biochemistry, Biophysics, and Molecular Biology, Iowa State University, Ames, Iowa 50011, USA. [2]Department of Biochemistry and Cell Biology, Rice University, Houston, Texas 77251-1892, USA. [3]These authors contributed equally to this work. Correspondence should be addressed to Y.-K.S. (colishin@iastate.edu).

Published online 10 April 2005; doi:10.1038/nsmb921

© 2005 Nature Publishing Group http://www.nature.com/nsmb

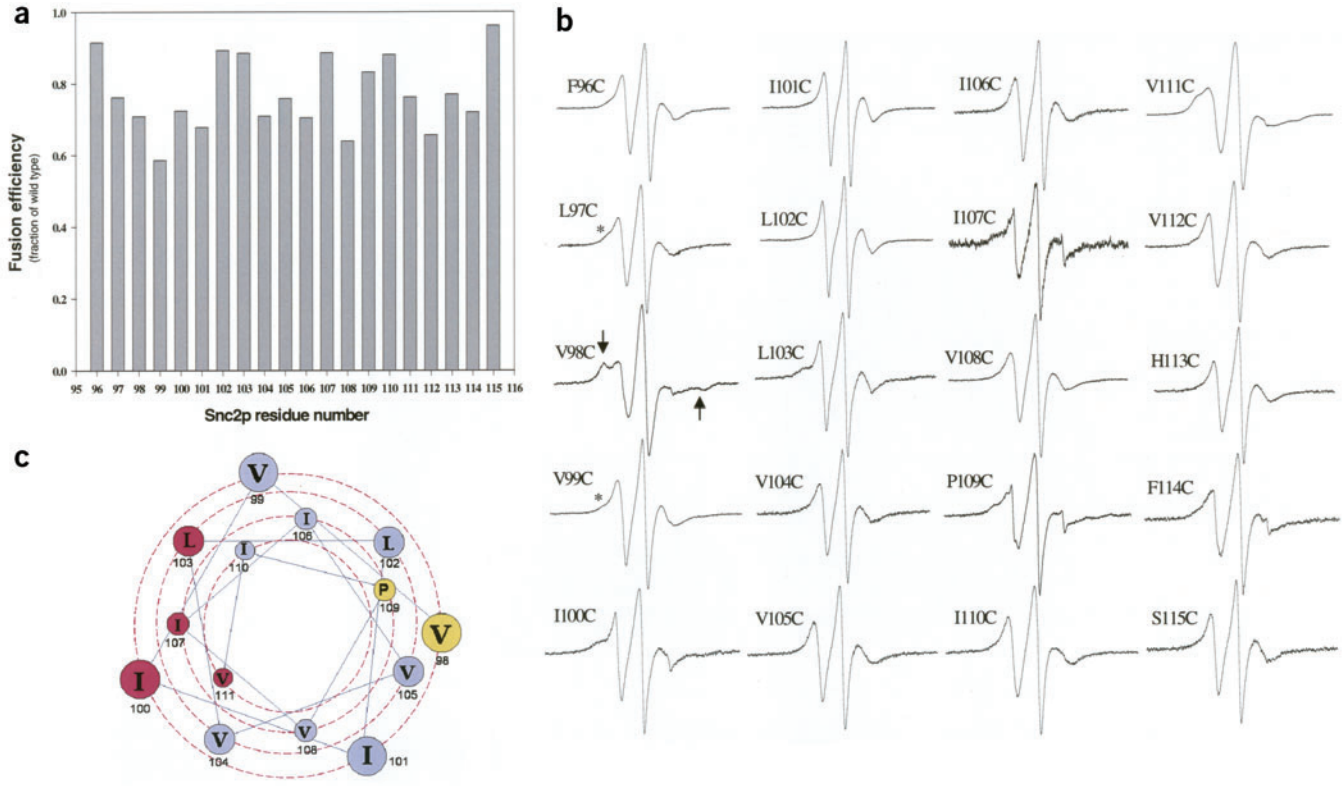

Figure 1 Site-directed spin labeling and the EPR analysis of Snc2p. (**a**) Fusion activity of spin-labeled Snc2p mutants measured by an *in vitro* fusion assay[14]. The fusion activity of each mutant was normalized against that of the wild type. The reconstitution efficiency, determined by EPR[24], was nearly the same for all mutants (~60%). The fusion assay for every mutant was repeated three times. (**b**) Room temperature EPR spectra of the spin-labeled Snc2p mutants. The arrow indicates the broad component, suggestive of the tertiary interactions. (**c**) Helical wheel diagram of the Snc2p TMD. Positions 100, 103, 107 and 111, which show the tertiary interactions on one side of the helix are red and 98 and 109, which show the interactions on the other side of the helix, are yellow. We also noticed some weak tertiary interactions (asterisk in **b**) at positions 97 and 99.

observed an immobilized spectrum for positions 98 and 109, indicating some further interactions on the other side of the helix.

Transmembrane structure of v-SNARE Snc2p

The EPR saturation method[23] was used to measure accessibility and characterize the structure of Snc2p in the membrane. We measured the accessibility of the nitroxide to a water-soluble paramagnetic reagent, nickel-ethylenediaminediacetic acid (NiEDDA) (W_{NiEDDA}) (**Fig. 2a**), to estimate the extent of seclusion of the spin-labeled site from the aqueous phase. We also determined the accessibility to a nonpolar paramagnetic reagent, molecular oxygen (W_{O2}) (**Fig. 2a**), to probe the immersion into the nonpolar membrane interior.

The W_{NiEDDA} values are low whereas the W_{O2} values are high, characteristic of nitroxides exposed to the lipid phase. The ratio of W_{O2} to

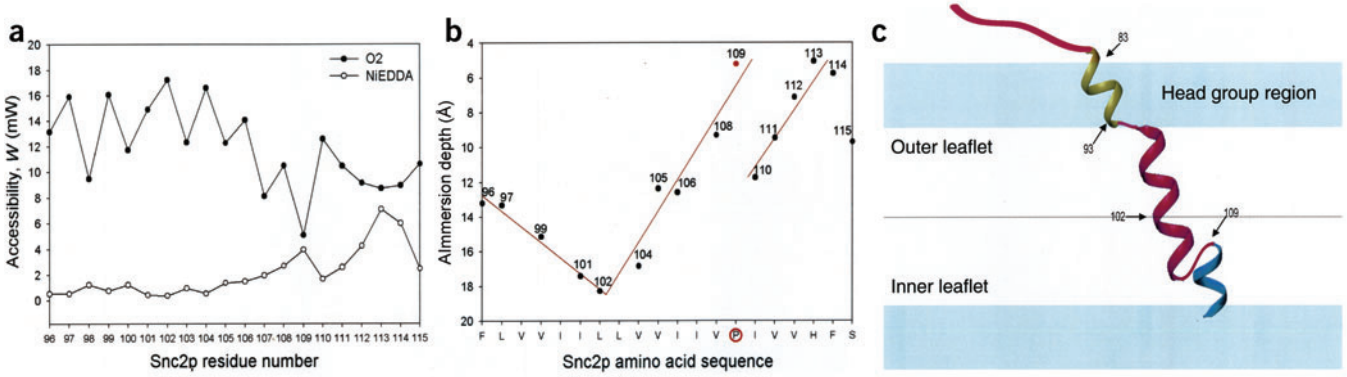

Figure 2 Structural determination of the Snc2p TMD using EPR. (**a**) Accessibility parameters W_{O2} and W_{NiEDDA}. Typical W_{NiEDDA} and W_{O2} values for the fully lipid-exposed residues are around 2 and 12 mW, respectively. (**b**) Membrane immersion depths. Residues 98, 100, 103 and 107 were not included in the analysis. Pro109 is circled and highlighted red. (**c**) A structural model. The head group region of the bilayer is blue. The structure preceding position 96 was adopted from previous work[24,25]. Residues 93–108 (purple) are in the acyl chain region. Residues following Pro109 were modeled as a short α-helix. Amino acids 93–108 span ~22 Å (1.37 Å per residue on average), which is equivalent to a 24° tilt, assuming 1.5 Å per residue for a straight α-helix.

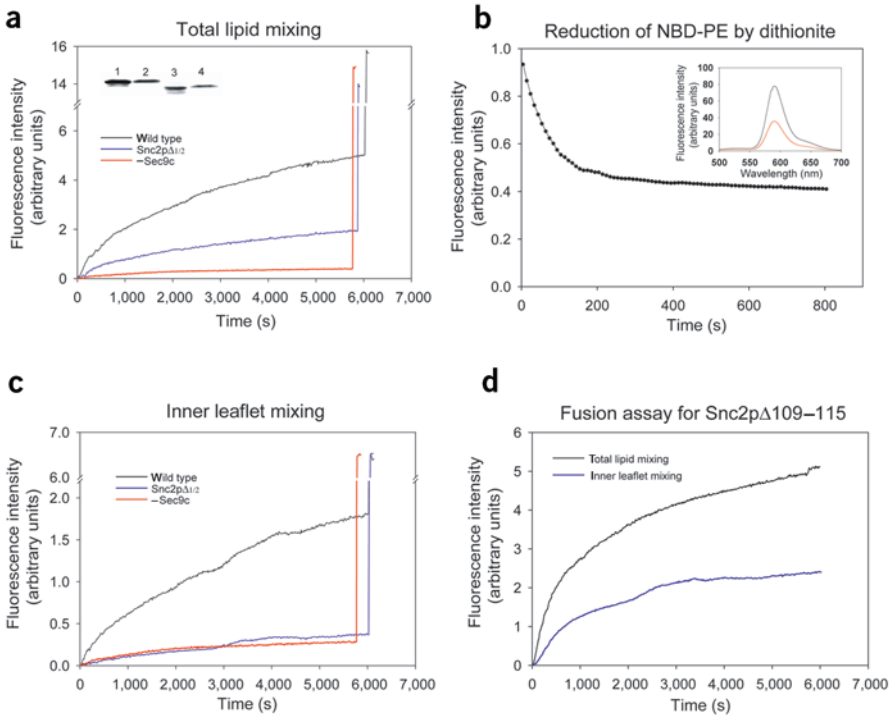

Figure 3 Total and inner leaflet lipid mixing for Snc2p and its mutants. (**a**) Total lipid mixing assay. Fluorescence intensities are plotted versus time for experiments in which wild-type Snc2p was used (black) and Snc2p$\Delta_{1/2}$ was used as v-SNARE (blue). The red line is a control in the absence of Sec9c. The maximal fluorescence intensity (MFI) was obtained by adding 0.25% *n*-dodecylmaltoside (sudden jumps at the ends)[14]. The percent values of MFI for Snc2p and Snc2p$\Delta_{1/2}$ are approximately 31% and 12%, respectively. Inset, the reconstitution efficiency was estimated using the SDS-PAGE analysis; wild-type Snc2p before (lane 1) and after reconstitution (lane 2), and Snc2p$\Delta_{1/2}$ before (lane 3) and after reconstitution (lane 4). The reconstitution efficiencies measured by densitometry were 60% for the wild type and 64% for the mutant. The Snc2p$\Delta_{1/2}$ bands seemed weaker owing to poorer staining than for the wild type, although the same amounts were used for lanes 1 and 3. (**b**) Reduction of NBD-PE by dithionite. The reduction of NBD-PE in donor vesicles by dithionite was measured as a loss of FRET between NBD and rhodamine (excitation at 460 nm and detection at 590 nm). Inset, florescence spectra before (black) and after dithionite treatment (red). (**c**) Inner leaflet mixing assay. Comparison of the inner leaflet mixing when Snc2p is used as v-SNARE (black) with that when Snc2p$\Delta_{1/2}$ was used (blue). The red line is the control in the absence of Sec9c. The percent values of MFI were about 28% for Snc2p and 3% for Snc2p$\Delta_{1/2}$, respectively. The red line is a control in the absence of Sec9c when Snc2p$\Delta_{1/2}$ was used, which shows ~3% of MFI. (**d**) Total lipid (black) and inner leaflet (blue) mixing assays for the Snc2p mutant lacking residues 109–115 (Snc2pΔ109–115). The percent of MFI was ~30% for both assays. The molar lipid/protein ratio was 200:1 for all experiments.

© 2005 Nature Publishing Group http://www.nature.com/nsmb

W_{NiEDDA} is quantitatively proportional to the immersion depth of spin label, and immersion depths were calculated from this ratio compared to a standard curve[23,24] (**Fig. 2b**). Because the depth-to-ratio relationship holds only for fully lipid-exposed nitroxides[23], we excluded mutants V98C, I100C, L103C, I107C and V111C in this analysis. Additionally, we included the results for residues Gln83–Leu95 from the previously published work[25] to cover the full TMD.

These results suggest that residues Gln83–Leu102 reside in the outer monolayer of the liposome membrane, whereas residues Leu103–Ser115 are embedded in the inner monolayer. As expected, we observed a break in the depth profile at Pros109. This analysis also revealed that the main helical segment (residues Met93–Val108) is tilted ~24° with respect to the membrane normal (**Fig. 2c**).

Hemifusion in SNARE-mediated membrane fusion

The EPR-based structural model of the Snc2p TMD guided us to design experiments to explore the roles of the TMD in membrane fusion. Previous work with lipid-anchored SNAREs suggests that the immersion depth of the hydrophobic anchor is an important determinant of membrane fusion[19], which is in accord with work using a transmembrane deletion mutant of HA[9].

To test this idea, we prepared the mutant Snc2p$\Delta_{1/2}$, which is truncated at residue 102 and does not contain amino acids 103–115. Since residue 102 is located in the middle of the bilayer (**Fig. 2b**) this mutant is predicted to span only the outer leaflet. The Snc2p$\Delta_{1/2}$ mutant was reconstituted into vesicles containing fluorescence dyes for the lipid mixing assay. Separate vesicles containing the t-SNARE heavy chain Sso1pHT were also prepared. When the two vesicle populations were mixed in the presence of soluble Sec9c, an increase in NBD fluorescence was observed indicating that lipid mixing had occurred (**Fig. 3a**, blue trace). Interestingly, the extent of the lipid mixing was about 35% of that observed for wild-type SNAREs (**Fig. 3a**, black trace). To show that lipid mixing was dependent on SNARE proteins, we omitted the t-SNARE light chain Sec9c since it is known that Sec9 is required for functional SNARE assembly[26]. When we mixed Snc2p-containing vesicles with Sso1pHT-containing vesicles in the absence of Sec9c, minimal lipid mixing was observed (**Fig. 3a**, red trace).

Given that similar amounts of the Snc2p$\Delta_{1/2}$ mutant protein are reconstituted compared with wild type (**Fig. 3a**, inset), one possibility to explain the >50% reduction in lipid mixing with Snc2p$\Delta_{1/2}$ is hemifusion rather than full fusion. A hallmark of hemifusion is that the outer monolayer of the membrane (~50% of total membrane) merges while the inner monolayer remains intact and does not mix[6].

To directly measure inner leaflet mixing, we treated the Snc2p-reconstituted vesicles with sodium dithionite[27]. Under controlled conditions, sodium dithionite reduces the NBD attached to a lipid head group in the outer leaflet to a nonfluorescent derivative while leaving NBD in the inner leaflet largely unaffected (**Fig. 3b**). Lipid mixing, specific to the inner leaflet, can be measured with dithionite-treated donor vesicles. When we mixed dithionite treated wild type Snc2p vesicles with Sso1pHT vesicles in the presence of Sec9c, inner leaflet mixing was seen (**Fig. 3c**, black trace). In contrast, no lipid mixing was observed when we incubated dithionite-treated Snc2p$\Delta_{1/2}$ vesicles with vesicles from t-SNARE complex (**Fig. 3c**, blue trace), strongly suggesting that the inner leaflets of two membranes did not merge. Taken together, the results for Snc2p$\Delta_{1/2}$ are consistent with hemifusion.

Notably, both Snc1p and Snc2p have a proline residue at the same location within the TMD. This proline is not conserved in other members of the v-SNARE family and is located in the inner layer of the membrane. To investigate the functional importance of amino

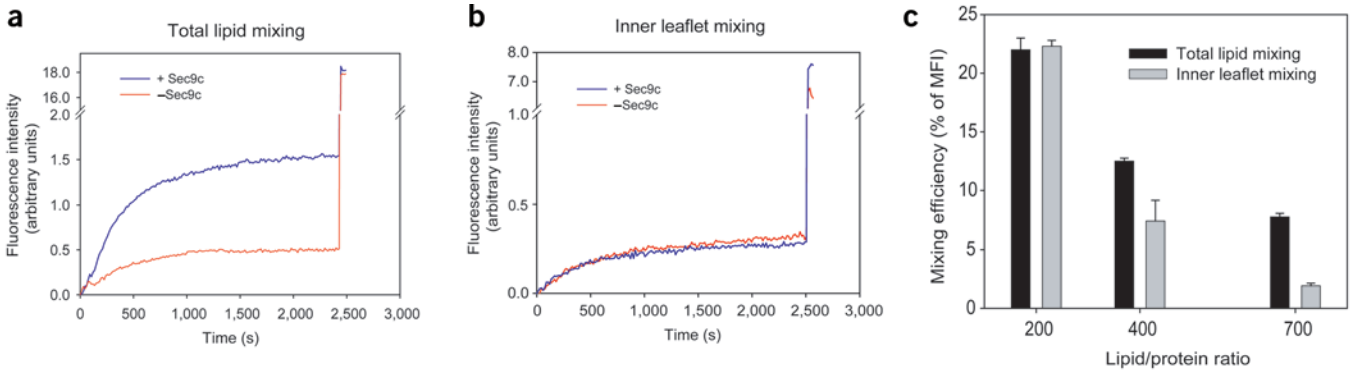

Figure 4 Total and inner leaflet lipid mixing assays at low protein concentrations. (**a**) Total lipid mixing assay for the 700:1 molar lipid/protein ratio (blue line). Both v-SNARE and t-SNARE are reconstituted to the vesicles containing DOPC, DOPS and DOPE (molar ratio of 0.35:0.35:0.3). The red line is the control without Sec9c. (**b**) Inner leaflet mixing assay for the 700:1 lipid/protein ratio (blue line). The red line is the control without Sec9c. (**c**) The mixing efficiency (the percent of MFI) as a function of the lipid/protein ratio. The bars represent the fluorescence intensity change at 2,500 s. As controls, the fluorescence changes were measured in the absence of Sec9c. The controls, which were not the direct consequence of membrane fusion, were subtracted from the data in the analysis to calculate the percent of MFI. The error bars are s.d. of at least three independent measurements.

© 2005 Nature Publishing Group http://www.nature.com/nsmb

acids following Pro109, we made a Snc2p mutant lacking amino acids 109–115. When examined with the total lipid mixing assay, the deletion mutant had fusion activity very similar to that of wild type, which was ~30% of the maximum fluorescence intensity (MFI) obtained by adding 0.25% *n*-dodecylmaltoside (**Fig. 3d**, black trace). Furthermore, inner leaflet mixing produced a fluorescence signal ~40% of the total lipid mixing (**Fig. 3d**, blue trace), strongly indicating that the region below Pro109 is not necessary for full fusion.

Hemifusion for wild-type SNAREs

Our results show that a deletion mutant of the v-SNARE Snc2p mediates hemifusion similarly to influenza HA deletion mutants[9]. Membrane fusion with influenza HA can be also trapped at hemifusion when the concentration of HA on the membrane surface is sufficiently low[28,29]. If hemifusion is an intermediate in the fusion pathway for SNARE proteins, then we might be able to observe hemifusion with wild-type SNAREs when the surface concentration of SNAREs is also low.

To test this hypothesis, we carried out the total lipid mixing assay and the inner leaflet lipid mixing assay at 200:1, 400:1 and 700:1 molar lipid/protein ratios (**Fig. 4**). For these experiments, we reconstituted SNAREs into vesicles that also contain phosphatidylethanolamine (PE), a lipid that is proposed to stabilize hemifusion owing to its preference for the negative membrane curvature[6]. At our normal 200:1 ratio, both assays showed the same mixing efficiency, indicating that all fusion events were at full fusion (**Fig. 4c**). However, at the lower protein levels, the mixing efficiency of the total lipid mixing assay was higher than that of the inner leaflet mixing assay, indicating that some fusion was limited to hemifusion, similar to the case with flu HA. At a 400:1 protein/lipid molar ratio, ~35% of the total lipid mixing signal was derived from hemifusion (the ratio of total lipid mixing versus inner leaflet mixing), whereas, at 700:1, ~75% of the total lipid mixing signal was derived from hemifusion. These results suggest that hemifusion could be an intermediate for SNARE-induced membrane fusion (**Fig. 4c**). In control experiments, when we mixed Snc2p-containing vesicles with Sso1pHT-containing vesicles without Sec9c, minimal lipid mixing was observed for all three lipid/protein ratios (red traces in **Fig. 4a**,**b**). Another control in the absence of all three SNARE proteins showed a nearly identical background to the control without Sec9c (**Supplementary Fig. 1** online). However, we could not trap hemifusion when we used the usual POPC/DOPS (75/25) vesicles even at the 700:1 lipid/protein ratio.

DISCUSSION

The observation of hemifusion for SNARE-mediated membrane fusion seems inconsistent with a mechanistic model based on a gap junction–like protein pore[15]. Although our results support a role for the TMD of the SNARE proteins in membrane fusion, this role is unlikely to be exclusively as a protein pore. If the protein pore model were valid, the protein-lined pore would have to be resealed to create hemifusion before advancing to a larger pore, which is quite unlikely although not impossible. Furthermore, the fact that full fusion can be achieved without a proteinaceous transmembrane domain *in vitro*[19] and *in vivo*[16] directly contradicts a protein pore model.

The experimental evidence for the protein pore is the electrophysiological observation of the conductance for the t-SNARE-containing membrane[15]. In this model, it is postulated that v-SNARE might form a similar pore in the membrane. For yeast v-SNARE Snc2p, we observed immobilized spectra or some tertiary interactions at six different positions, indicating that the TMD has a tendency to form oligomers. However, for all positions, W_{NiEDDA} values are low, whereas W_{O2} values are quite high, strongly suggesting that they are partially or fully exposed to the lipid phase. Therefore, it is unlikely that the Snc2p TMD forms an aqueous pore in the membrane, although we cannot rule out the possibility that a small fraction of Snc2p molecules form protein pores. Furthermore, the addition of nitroxide spin labels throughout the TMD only modestly affected the fusion activities of spin-labeled mutants (**Fig. 1a**). These data indicate either that a TMD-lined pore does not exist, or that bulky nitroxide spin labels do not affect its function.

In SNARE-induced membrane fusion, coiled-coil formation has been postulated to be a key step that generates the necessary force to overcome the fusion energy barriers[30,31]. The core complex has been shown to be structurally coupled to the membranes[32,33]. The structural coupling between the coiled coil and the TMDs would facilitate force transfer to the TMDs, which would then promote the merger of the outer leaflets (hemifusion) and, subsequently, the merger of the inner leaflets (full fusion). For the Snc2p$\Delta_{1/2}$ mutant, which can only span the outer leaflet, energy would not be effectively transferred to the inner leaflet, leading to hemifusion but not full fusion.

A previous study examined the fusion activities of several flu HA mutants for which the TMD was systematically deleted[9], and also observed hemifusion for HA mutants that had the short membrane domain. For mutants with a longer membrane domain, however, full fusion was

detected. Those results agree well with our results with SNAREs, supporting the idea that hemifusion might be a common intermediate along the fusion pathways.

For flu HA, another previous study proposed the "boomerang mechanism"[34], in which the fusion peptide–TMD interaction is a key component. In this model, it is hypothesized that a fusion peptide–TMD interaction provides the driving force for the deformation of the membrane required for the advancement from hemifusion to the fusion pore. It is unclear, however, whether such a mechanism is operative for SNARE-induced membrane fusion. It is possible that the TMD of the v-SNARE interacts with the TMD of the t-SNARE, which might facilitate the completion of fusion in a similar fashion. A v-SNARE mutant with a sufficiently short TMD would certainly lose its ability to fully interact with the TMD of the t-SNARE. It is also conceivable that the short membrane domain of Snc2p$\Delta_{1/2}$ acts like a fusion peptide. The short hydrophobic membrane domain of Snc2p$\Delta_{1/2}$ may be mobile in the plane of the membrane; this could disturb the surface structure of the membrane sufficiently enough to induce hemifusion.

In summary, we have identified hemifusion for SNARE-induced membrane fusion, raising the possibility that hemifusion be a common intermediate for all membrane fusion events.

METHODS

Protein sample preparation. Plasmid construction, mutagenesis, protein expression, purification and spin labeling for yeast SNAREs have been described[25]. Briefly, v-SNARE Snc2p (amino acids 1–115, neuronal synaptobrevin analog) and a truncated version of t-SNARE Sso1p (neuronal syntaxin analog) Sso1pHT (amino acids 185–290), for which the N-terminal α-helical Habc domain was deleted, were expressed as N-terminal glutathione *S*-transferase (GST) fusion proteins. The other t-SNARE component, Sec9c (amino acids 401–651 of Sec9, neuronal SNAP-25 analog), was expressed as C-terminal His_6-tagged protein. To place a unique cysteine for spin labeling, native Cys266 of Sso1pHT and Cys94 of Snc2p were replaced with alanines. The QuikChange mutagenesis kit (Stratagene) was used to generate point mutants. The truncated versions of Snc2p lacking parts of TMD were generated by introducing a stop codon at desired positions. DNA sequences were confirmed by the Iowa State University DNA Sequencing Facility.

Recombinant proteins were expressed in *Escherichia coli* Rosetta (DE3) pLysS (Novagen). The His_6-tagged protein Sec9c was purified by Ni-NTA agarose beads (Qiagen). After binding and washing, the protein was eluted by elution buffer (PBS with 250 mM imidazole, pH 8.0). GST fusion proteins were purified by affinity chromatography using glutathione-agarose beads (Sigma).

Cysteine mutants of Snc2p were spin-labeled while the protein was still bound to beads. A ~20-fold molar excess of (1-oxyl-2,2,5,5-tetramethylpyrrolinyl-3-methyl) methanethiosulfonate spin label (MTSSL) was added to the column, and the reaction mixture was left overnight at 4 °C. Unreacted MTSSL was removed by washing with excess PBS buffer, pH 7.4, containing 0.2% (v/v) Triton X-100. The protein was cleaved by thrombin in cleavage buffer (50 mM Tris-HCl, 150 mM NaCl, 2.5 mM $CaCl_2$, pH 8.0, 0.2% (v/v) Triton X-100). Purified proteins were examined by SDS-PAGE (data not shown) and the purity was at least 90% for all proteins. The spin-labeling efficiency was estimated by comparing the protein concentration obtained from the Bio-Rad DC protein assay and the spin concentration determined with EPR.

Membrane reconstitution. The mixture of POPC, DOPS (molar ratio of 75:25) or DOPC/DOPS/DOPE (molar ratio of 35:35:30) in chloroform was dried in vacuum and was resuspended in a buffer (50 mM Tris-HCl, 150 mM NaCl, 2.5 mM $CaCl_2$, pH 8.0) to make the total lipid concentration ~100 mM. Large unilamellar vesicles (100 nm in diameter) were prepared using Extruder (Avanti Polar Lipids). Proteins were then mixed with vesicles at a desired protein/lipid molar ratio. The detergent in the samples was removed by the Bio-beads method. The samples were treated with Bio-beads SM2 (Bio-Rad). Bio-beads were first washed extensively with deionized water. After washing, water was decanted from Bio-beads as much as possible after centrifugation. Bio-beads were then directly added to the sample in the ratio of 200 mg per milliliter of mixed solution. After 30 min of nutation, Bio-beads were removed from the sample by removing the solution using a pipette after centrifugation at 5,000*g*. The same procedure was repeated three times. The samples were then dialyzed against 2 l dialysis buffer (25 mM HEPES, 100 mM KCl, pH 7.4) at 4 °C overnight to remove any trace amount of detergent that might interfere with the fluorescence measurement. After dialysis, the solution was centrifuged at 10,000*g* to remove protein and lipid aggregates. Reconstitution efficiency was estimated by determining the protein concentrations before and after reconstitution with EPR. For all samples, the efficiency was ~60%. The reconstituted vesicles were examined with negative-staining EM as described[25] and the average size was ~100 nm (data not shown).

EPR data collection and accessibility measurements. A Bruker ESP 300 EPR spectrometer equipped with a loop-gap resonator was used to obtain the EPR spectra. The details of data collection and analysis have been described[35,36]. Briefly, power saturation curves were obtained from the peak-to-peak amplitude of the central line ($M = 0$) of the first derivative EPR spectrum as a function of incident microwave power in the range 0.1–40 mW. For each mutant, three power saturation curves were obtained after equilibration: (i) with N_2, (ii) with air (O_2), and (iii) with N_2 in the presence of 200 mM NiEDDA. From saturation curves, the microwave power $P_{1/2}$, where the first-derivative amplitude is reduced to one-half of its unsaturated value, was calculated. The quantity $\Delta P_{1/2}$ is the difference in $P_{1/2}$ values in the presence and absence of a paramagnetic reagent. $\Delta P_{1/2}$ (in units of mW) is considered to be equivalent to the accessibility, W[35]. EPR saturation experiments were done at 22 °C.

Total lipid mixing fluorescence assay. To assay the total lipid mixing using fluorescence, Snc2p was reconstituted into the donor vesicles containing POPC, DOPS, NBD-PE and rhodamin-PE in the molar ratio of 72:25:1.5:1.5. SSo1pHT was reconstituted into separate vesicles containing POPC and DOPS in the molar ratio 75:25. To measure the lipid mixing, Snc2p-reconstituted vesicles were mixed with Sec9c and Sso1pHT-reconstituted vesicles according to the aimed ratio. The final solution contained ~1 mM lipids. Fluorescence was measured at excitation and emission wavelengths of 465 and 530 nm, respectively. Fluorescence changes were recorded with a Varian Cary Eclipse model fluorescence spectrophotometer using a quartz cell of 100 μl with a 2-mm path length. The MFI was obtained by adding 0.25% (v/v) *n*-dodecylmaltoside[19]. All lipid mixing experiments were carried out at 35 °C.

Inner layer lipid mixing assay. The inner layer lipid mixing assay was modified from a described method[28]. The donor vesicles with fluorescence probes exclusively in the inner layer were prepared before the lipid mixing assay. The method is based on the fact that the sodium dithionite reacts more rapidly with NBDs in the outer leaflet than those in the inner leaflet. By controlling the time and amount of dithionite, the reaction could be largely limited to the outer leaflet. Small aliquots of 200 mM sodium dithionite in 50 mM Tris buffer, pH 10, sufficient to reduce slightly more than 50% of NBD-PE, were added to the Snc2p-reconsitituted vesicles. The reaction was monitored at room temperature by scanning the fluorescence signal for 15 min from 500 to 700 nm with excitation at 460 nm. These vesicles without NBDs in the outer leaflet were subject to the lipid mixing assay described above.

Note: Supplementary information is available on the Nature Structural & Molecular Biology website.

ACKNOWLEDGMENTS

Support for this work was provided by the US National Institutes of Health (Y-.K.S) and the US National Science Foundation and the Robert A. Welch Foundation (J.A.M.).

COMPETING INTERESTS STATEMENT

The authors declare that they have no competing financial interests.

Received 14 January; accepted 10 March 2005
Published online at http://www.nature.com/nsmb/

1. White, J.M. Membrane fusion. *Science* **258**, 917–924 (1992).
2. Skehel, J.J. & Wiley, D.C. Coiled coils in both intracellular vesicle and viral membrane fusion. *Cell* **95**, 871–874 (1998).
3. Chan, D.C. & Kim, P.S. HIV entry and its inhibition. *Cell* **93**, 681–684 (1998).
4. Jahn, R., Lang, T. & Sudhof, T.C. Membrane fusion. *Cell* **112**, 519–533 (2003).

© 2005 Nature Publishing Group http://www.nature.com/nsmb

5. Earp, L.J., Delos, S.E., Park, H.E. & White, J.M. The many mechanisms of viral membrane fusion proteins. *Curr. Top. Microbiol. Immunol.* **285**, 25–66 (2005).
6. Chernomordik, L.V. & Kozlov, M.M. Protein-lipid interplay in fusion and fission of biological membranes. *Annu. Rev. Biochem.* **72**, 175–207 (2003).
7. Kemble, G.W., Danieli, T. & White, J.M. Lipid-anchored influenza hemagglutinin promotes hemifusion, not complete fusion. *Cell* **76**, 383–391 (1994).
8. Melikyan, G.B., Markosyan, R.M., Roth, M.G. & Cohen, F.S. A point mutation in the transmembrane domain of the hemagglutinin of influenza virus stabilizes a hemifusion intermediate that can transit to fusion. *Mol. Biol. Cell* **11**, 3765–3775 (2000).
9. Armstrong, R.T., Kushnir, A.S. & White, J.M. The transmembrane domain of influenza hemagglutinin exhibits a stringent length requirement to support the hemifusion to fusion transition. *J. Cell Biol.* **151**, 425–437 (2000).
10. Yang, L. & Huang, H.W. Observation of a membrane fusion intermediate structure. *Science* **297**, 1877–1879 (2002).
11. Rothman, J.E. Mechanisms of intracellular protein transport. *Nature* **372**, 55–63 (1994).
12. Chen, Y.A., Scales, S.J., Patel, S.M., Doung, Y.C. & Scheller, R.H. SNARE complex formation is triggered by Ca^{2+} and drives membrane fusion. *Cell* **97**, 165–174 (1999).
13. Weber, T. *et al.* SNAREpins: minimal machinery for membrane fusion. *Cell* **92**, 759–772 (1998).
14. McNew, J.A. *et al.* Compartmental specificity of cellular membrane fusion encoded in SNARE proteins. *Nature* **407**, 153–159 (2000).
15. Han, X., Wang, C.T., Bai, J., Chapman, E.R. & Jackson, M.B. Transmembrane segments of syntaxin line the fusion pore of Ca^{2+}-triggered exocytosis. *Science* **304**, 289–292 (2004).
16. Grote, E., Baba, M., Ohsumi, Y. & Novick, P.J. Geranylgeranylated SNAREs are dominant inhibitors of membrane fusion. *J. Cell Biol.* **151**, 453–466 (2000).
17. Chernomordik, L.V. *et al.* Lysolipids reversibly inhibit Ca(2+)-, GTP- and pH-dependent fusion of biological membranes. *FEBS Lett.* **318**, 71–76 (1993).
18. Peters, C. *et al.* Trans-complex formation by proteolipid channels in the terminal phase of membrane fusion. *Nature* **409**, 581–588 (2001).
19. McNew, J.A. *et al.* Close is not enough: SNARE-dependent membrane fusion requires an active mechanism that transduces force to membrane anchors. *J. Cell Biol.* **150**, 105–117 (2000).
20. Hubbell, W.L., Gross, A., Langen, R. & Lietzow, M.A. Recent advances in site-directed spin labeling of proteins. *Curr. Opin. Struct. Biol.* **8**, 649–656 (1998).
21. Rabenstein, M.D. & Shin, Y.K. HIV-1 gp41 tertiary structure studied by EPR spectroscopy. *Biochemistry* **35**, 13922–13928 (1996).
22. McHaourab, H.S., Lietzow, M.A., Hideg, K. & Hubbell, W.L. Motion of spin-labeled side chains in T4 lysozyme. Correlation with protein structure and dynamics. *Biochemistry* **35**, 7692–7704 (1996).
23. Altenbach, C., Greenhalgh, D.A., Khorana, H.G. & Hubbell, W.L. A collision gradient method to determine the immersion depth of nitroxides in lipid bilayers: application to spin-labeled mutants of bacteriorhodopsin. *Proc. Natl. Acad. Sci. USA* **91**, 1667–1671 (1994).
24. Macosko, J.C., Kim, C.H. & Shin, Y.K. The membrane topology of the fusion peptide region of influenza hemagglutinin determined by spin-labeling EPR. *J. Mol. Biol.* **267**, 1139–1148 (1997).
25. Chen, Y., Xu, Y., Zhang, F. & Shin, Y.K. Constitutive versus regulated SNARE assembly: a structural basis. *EMBO J.* **23**, 681–689 (2004).
26. Rossi, G., Salminen, A., Rice, L.M., Brunger, A.T. & Brennwald, P. Analysis of a yeast SNARE complex reveals remarkable similarity to the neuronal SNARE complex and a novel function for the C terminus of the SNAP-25 homolog, Sec9. *J. Biol. Chem.* **272**, 16610–16617 (1997).
27. Meers, P., Ali, S., Erukulla, R. & Janoff, A.S. Novel inner monolayer fusion assays reveal differential monolayer mixing associated with cation-dependent membrane fusion. *Biochim. Biophys. Acta* **1467**, 227–243 (2000).
28. Chernomordik, L.V., Frolov, V.A., Leikina, E., Bronk, P. & Zimmerberg, J. The pathway of membrane fusion catalyzed by influenza hemagglutinin: restriction of lipids, hemifusion, and lipidic fusion pore formation. *J. Cell Biol.* **140**, 1369–1382 (1998).
29. Mittal, A., Leikina, E., Chernomordik, L.V. & Bentz, J. Kinetically differentiating influenza hemagglutinin fusion and hemifusion machines. *Biophys. J.* **85**, 1713–1724 (2003).
30. Poirier, M.A. *et al.* The synaptic SNARE complex is a parallel four-stranded helical bundle. *Nat. Struct. Biol.* **5**, 765–769 (1998).
31. Sutton, R.B., Fasshauer, D., Jahn, R. & Brunger, A.T. Crystal structure of a SNARE complex involved in synaptic exocytosis at 2.4 Å resolution. *Nature* **395**, 347–353 (1998).
32. Kweon, D.H., Kim, C.S. & Shin, Y.K. The membrane-dipped neuronal SNARE complex: a site-directed spin labeling electron paramagnetic resonance study. *Biochemistry* **41**, 9264–9268 (2002).
33. Kweon, D.H., Kim, C.S. & Shin, Y.K. Insertion of the membrane-proximal region of the neuronal SNARE coiled coil into the membrane. *J. Biol. Chem.* **278**, 12367–12373 (2003).
34. Tamm, L.K. Hypothesis: spring-loaded boomerang mechanism of influenza hemagglutinin-mediated membrane fusion. *Biochim. Biophys. Acta* **1614**, 14–23 (2003).
35. Kweon, D.H., Kim, C.S. & Shin, Y.K. Regulation of neuronal SNARE assembly by the membrane. *Nat. Struct. Biol.* **10**, 440–447 (2003).
36. Kweon, D.H. *et al.* Probing domain swapping for the neuronal SNARE complex with electron paramagnetic resonance. *Biochemistry* **41**, 5449–5452 (2002).

© 2005 Nature Publishing Group http://www.nature.com/nsmb